# Critical behavior of $p(2\times2)$ oxygen on Ru(001): An example of four-state Potts critical exponents

H. Pfnür and P. Piercy*
*Physikdepartment E20, Technische Universität München, James Franck Strasse, D-8046 Garching, West Germany*
(Received 9 January 1989)

Atomic oxygen on the hexagonally close-packed Ru(001) surface forms a $p(2\times2)$ structure on threefold-coordinated hcp sites. The critical behavior of the structural order-disorder phase transition was studied with low-energy electron diffraction at a relative coverage $\Theta=0.25$. Quantitative profile analysis of superstructure beams together with measurements of integrated and peak intensities as a function of temperature in the reduced temperature range $0.004<t<0.1$ were used to determine the exponents $\alpha$, $\beta$, $\gamma$, and $\nu$. They agree within 3% to 10% with the values of the two-dimensional four-state Potts universality class. Conditions and limitations of this determination are discussed.

## I. INTRODUCTION

Studies of thermodynamical properties of two-dimensional systems have attracted much attention both by experimentalists and theorists during recent years.[1] Experiments mainly concentrate on static thermodynamic properties such as phase diagrams and, in a few cases, static critical behavior. The information contained in such studies is twofold: First, phase diagrams are a main source of information about lateral interactions. In the simplest cases they can be described by lattice-gas models[2] with effective interactions at discrete sites. Chemisorbed adlayers provide a great variety of examples for which this description is applicable.[3] Second, tests of critical behavior of continuous phase transitions in two dimensions (2D) are particularly interesting, as deviations from classical mean-field behavior are expected to be strongest in 2D.[4] Structural order-disorder phase transitions of commensurate adlayers are easiest to control, and appear to be the simplest test systems in strictly 2D, if complications like dissolution of adatoms in the bulk can be neglected. Continuous phase transitions depend only on dimensionality and on the symmetry change between ordered and disordered phase.[5] Symmetry requirements for a phase transition to be continuous (or first order otherwise) are summarized in the "Landau rules,"[6] which for commensurate order-disorder transitions become particularly simple in 2D.[7] The validity of the "Landau rules" in 2D has not been extensively tested yet by experiment.[7] Following the first and third Landau rule, order-disorder transitions of adsorbed commensurate layers are predicted to fall into only a small number of universality classes.[8] The symmetry of the disordered system and the symmetry change, described by the order parameter, determines to which universality class a transition belongs. Therefore, the symmetry of the *disordered* phase must be known as well as that of the ordered phase. Whereas the latter can be determined reliably also in 2D by well-established methods like dynamical low-energy electron diffraction (LEED)-*IV* analysis,[9] determination of the former is more difficult. The $p(2\times2)$ structure on a triangular or hexagonal surface is particularly interesting because it has the largest unit cell which, according to the "Landau rules," can have a continuous order-disorder transition in 2D.[8] If the adlayer is adsorbed on a high-symmetry site, this order-disorder transition should fall into the four-state Potts universality class.[8] We show in this paper for the case of atomic oxygen on Ru(001) at a coverage of 0.25 (measured with respect to the substrate density) that a continuous transition can actually occur for this type of unit cell and that the measured exponents are, within the error limits, those of the four-state Potts universality class.

Although the number of possible candidates for studies of critical phenomena in 2D by simple order-disorder phase transitions is huge,[10] only a small number of quantitative experimental investigations of two-dimensional critical phenomena has been reported so far. These comprise clean reconstructed surfaces,[11,12] chemisorbed[13–17] as well as physisorbed adlayers.[18–22] They all fall into the universality classes of either the Ising, the three-state Potts, or the XY model with cubic anisotropy. No successful test in the four-state Potts class in 2D has been reported so far.[17] The many possible complications of perfect 2D order, like defects and bulk dissolution or the occurrence of first-order transitions, but also unknown structural properties of the disordered phase, might be reasons for this small number of investigations.

The chemical, structural, and kinetic properties of the system O/Ru(001) have been investigated by several authors (Refs. 23–29). Oxygen is only dissociatively adsorbed at and above room temperature[24] and forms only apparent $(2\times2)$ structures. During adsorption at room temperature the LEED intensity of oxygen induced superstructure beams exhibits two maxima, the first at half, the second at saturation coverage.[23] From high-resolution electron-energy-loss spectroscopy (HREELS) measurements[26] and LEED investigations on a stepped Ru(001) surface,[29] there is strong evidence that the intensity maximum at saturation corresponds to the formation

 

of three domains of a $p(2\times1)$ structure instead of a honeycomb structure which would also be possible from the LEED pattern. A saturation coverage at room temperature of $\Theta=0.5$ is also consistent with a comparison of O 1*s* XPS intensities of a saturated oxygen layer with that of a completed $\sqrt{3}\times\sqrt{3}R\,30°$-ordered layer of CO on this surface.[30] The first maximum at half-saturation coverage then corresponds to $\Theta=0.25$, where a $p(2\times2)$ structure must be formed. The work function changes almost linearly up to this coverage with an abrupt change of slope for higher $\Theta$, corresponding to an increase of effective dipole moment per added atom by a factor of 3.

In this paper, we concentrate on the determination of critical exponents. The phase diagram, a necessary prerequisite for the determination of critical exponents, was published in Ref. 31. It shows two maxima at relative coverages 0.5 and 1 with $T_c$ at 754 and 555 K, respectively. They coincide with the maxima in LEED superstructure intensity and must therefore correspond to completion of the $p(2\times2)$ structure at $\Theta=0.25$ and of the $p(2\times1)$ structure at $\Theta=0.5$. A detailed discussion of phase diagram and effective lateral interactions is postponed to a planned forthcoming publication.[32] Here we describe the determination of critical exponents of the $p(2\times2)$ order-disorder phase transition at $\Theta=0.25$. In order to avoid Fisher renormalization,[33] critical exponents were determined for the completed $p(2\times2)$ structure at $\Theta=0.25$, where $T_c$ is maximal and the order-disorder phase transition can be shown to be continuous. From a profile analysis of several superstructure beams, we show that these exponents are consistent with exponents of the four-state Potts universality class. A preliminary report of these results has been published recently.[34]

## II. EXPERIMENTAL

Our experiments were carried out in an UHV chamber at a base pressure of $2\times10^{-11}$ mbar with a four-grid LEED system equipped with a Faraday cup, movable both in polar and azimuthal directions. Primary electron currents of 60–100 nA at normal incidence were used and stabilized to 0.1%. Diffraction spot profiles and peak intensities were measured in polar direction of the Faraday cup with a round aperture subtending a (polar) angle of 0.5°, while for measurements of integrated intensities an aperture of 3.4° was used. For profiles, the reproducibility of FWHM was always better than 0.05°. A master-slave combination of microcomputers controls both polar and azimuthal motions of the Faraday cup, measures and stores data. Data are then transferred to a $\mu$VAX system for analysis.

The resistive sample heating, chopped alternately with the LEED current at 12.5 Hz, is controlled by another microcomputer. Temperature measurement is done via a chromel-alumel thermocouple with a resolution of 0.025 K. The sample was mounted by a set of wires (one Ir, two W–3 at.% Re, 0.5-mm diameter $\phi$, free length 4 mm) spot welded to the rear of the sample. These were again spot welded to the sample holder. The manipulator has two rotations, one around the surface normal, the other parallel to the surface, and allows adjustments of the sample to line up the axes of rotation. The ruthenium crystal was cut by spark erosion, oriented within 0.2°, and polished with diamond pastes down to 0.25 $\mu$m grain size. Cleaning was done by several hundred heating and cooling cycles between 400 and 1500 K in $5\times10^{-7}$ mbar oxygen. This extensive procedure also seems to improve the quality of the clean surface, as seen by the LEED reflectivity.

## III. DATA EVALUATION AND RESULTS

### A. Coverage calibration

Relative coverages at 400 K were determined by measuring relative peak to peak Auger intensities of the 520-eV oxygen KLL Auger transition in $dN/dE$ spectra with the retarding field analyzer as a function of exposure. The sample was dosed by a background pressure of $(1-3)\times10^{-8}$ mbar. In agreement with findings by Madey *et al.*,[23] we found a constant sticking coefficient up to 80% of saturation coverage. For the same temperature we also measured LEED superstructure beam intensities as a function of exposure. Coverage was now calibrated versus exposure assuming that the first LEED intensity maximum corresponds to exactly $\Theta=0.25$. Exposures were reproducible within 2%, as was explicitly tested for the coverage of $\Theta=0.25$ by measuring the critical temperature $T_c$ and adjusting it to be maximum (see below). This coverage calibration assumes a defect-free surface. The coverage averaged over the whole crystal surface may deviate, therefore, though locally a perfect $p(2\times2)$ structure exists. Steps, however, often assumed to be the main limitation for long-range order, do not interrupt the order of oxygen on this surface.[35] The concentration of point defects, microfacets, etc. is unknown, but should be far below the maximum concentration of steps of 1.5% determined for a crystal surface prepared in the same way as the one used here.[13] Such defects can be important for the determination of exponents, causing finite-size rounding of the phase transition and shifts in $T_c$.[36]

At adsorption temperatures below 350 K and at the same pressures as above the adsorbed layer has to be annealed to 600 K before perfect order is achieved, as obvious from the LEED superstructure beam intensities as a function of temperature. After oxygen adsorption at 400 K and short heating to 600 K, LEED intensities of superstructure beams are fully reversible as a function of temperature. Explicit tests were carried out at constant coverage $\Theta=0.25$ for heating rates between 0.2 K/s and 10 K/s in the temperature range 200–950 K, ramping temperature both up and down. Differences in intensities were below 1%, those of $T_c$ within the uncertainty of its determination of 0.5 K. This contrasts with earlier reports of slow oxygen diffusion into deeper layers at temperatures above 700 K.[27] We note, however, slow oxygen removal from the surface which amounts to 1% of a monolayer over 30 min. This effect is almost temperature independent and was shown to be due to oxidation of CO adsorbed from the background pressure.

### B. Data evaluation of critical exponents

As discussed by Bartelt *et al.*,[37] the specific-heat exponent $\alpha$ can be evaluated from a low-resolution diffraction experiment, including all multiple diffraction effects. A low-resolution instrument such as a Faraday cup with large aperture is only sensitive to correlations of limited range. The singular part of the interaction energy depends on these finite as well as infinite range correlations in a way which has the same mathematical form as the LEED intensity integrated over a spot. Therefore, close to $T_c$ [or, equivalently, at small reduced $t=(T-T_c)/T_c$], the integrated intensity should decay with the critical exponent of the interaction energy, $1-\alpha$,

$$\int_{|\mathbf{q}-\mathbf{q}_c|<\mathbf{q}_m} d\mathbf{q}\, S(\mathbf{q}) = B_{\pm}|t|^{1-\alpha_{\pm}} + (A - Ct + \cdots) . \quad (1)$$

$A$ and $C$ are positive constants, the amplitudes $B_{\pm}$ and the exponents $\alpha_{\pm}$ refer to situations with $t>0$ and $t<0$, respectively. In case of infinite, nondistorted lattices this formula is valid, if for the integration radius in reciprocal space, $\mathbf{q}_m$, $q_m\xi \gg 1$ holds. The integral is then taken effectively over all correlations, which under the conditions chosen extend out to the correlation length $\xi$. As the correlation length $\xi$ decays $\sim|t|^{-\nu}$ this condition sets an upper limit in $t$ for the applicability of Eq. (1). For a finite system with a characteristic length $L$, deviations from Eq. (1) [as well as from Eq. (2) below] must be expected when the correlation length approaches $L$, thus limiting the applicability of Eq. (1) at small $|t|$ to $|t| \gg |t_{0\pm}|$ with $\xi(t_{0\pm})=L$.

The exponents $\beta$, $\gamma$, and $\nu$ can be extracted from the measured superstructure profiles[4,38] by parametrizing the ideal, i.e., deconvoluted, profile in the following way:

$$S(\mathbf{q},t) = I_0(t)\delta(\mathbf{q}-\mathbf{q}_0) + \chi_0(t)[1+(\mathbf{q}-\mathbf{q}_0)^2\xi^2(t)]^{-1} \quad (2)$$

with the correlation length $\xi \sim |t|^{-\nu}$, $I_0 \sim (-t)^{2\beta}$, and $\chi_0 \sim |t|^{-\gamma}$. The first term of Eq. (2) describes the Bragg peaks due to long-range order, whereas in the second the effects of critical scattering due to correlations of short-range order fluctuations are contained. This term is exact only if the Fisher exponent $\eta$ is zero.[4] However, this parametrization has the proper scaling form for small $\xi(q-q_0)$ and small $t$.[39] Deviations should be expected for large $\xi(q-q_0)$ [i.e., $\xi(q-q_0)\to\infty$ with $t\to0$, $q-q_0)\neq0$], depending on the size of exponent $\eta$ (Ref. 39). The parametrization of Eq. (2) can be expected to describe scaling of our data properly, as we use only data with $\xi(q-q_0)\leq 1$ for the evaluation of exponents, in agreement with our finding. In this limit unisotropies of $S$ can also be neglected.[38] As the fit to the experimental data shows (see Fig. 4), deviations from Lorentzian form are typically small for small differences $(q-q_0)$ from the Bragg peak position. Their consideration would in fact exceed the accuracy of our fitting procedure.

As already mentioned, instead of numerical deconvolutions we carried out fits to our experimental beam profiles. This procedure proved to be numerically much more stable and reliable than deconvolutions. In order to obtain correct results, especially for the peak heights $\chi_0$ above $T_c$, it turned out to be necessary to properly simulate a two-dimensional deconvolution in the fitting routine. We approximated the instrument function by a two-dimensional profile separable both in polar and azimuthal directions and assumed the deconvoluted Lorentzian profile to be isotropic. Measured low-temperature spot profiles in azimuthal and polar directions were taken as instrument functions. We adjusted the beam focus to obtain a transfer width of 175 Å in polar direction for a second-order superstructure beam at a primary energy of 65 eV, and accepted a 70% wider profile in the direction perpendicular. The azimuthal profile was approximated by a Gaussian of the measured width, and the convolution in azimuthal direction carried out with approximate analytic formulas tabulated in Ref. 40, whereas in polar direction the polar profile was directly taken as numerical input into the fitting procedure.

### C. Results

As already mentioned, critical exponents are defined for constant chemical potential, $\mu$. For constant coverage, the condition we have to work with, $\mu$ in general changes as a function of temperature, and exponents will be Fisher renormalized.[33] Renormalization is unimportant only at symmetry points of the phase diagram. Therefore, all our measurements are carried out at $\Theta=0.25$, which corresponds to the maximum in $T_c$.

As an example for measurements to determine the specific-heat exponent $\alpha$, the intensity of a second-order oxygen diffraction spot at $E_{\text{prim}}=65$ eV, integrated over 2.3% of the Brillouin zone, is shown in Fig. 1 as a function of temperature, together with a fit according to Eq. (1). The experimental curve shown is already divided by

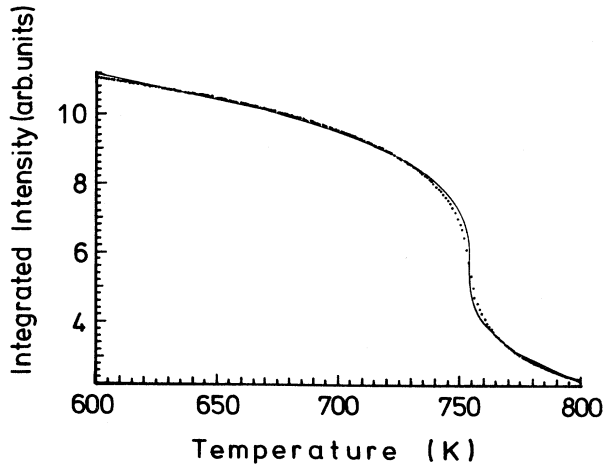


FIG. 1. Integrated intensity of an oxygen-induced $(\frac{1}{2},\frac{1}{2})$ superstructure beam as a function of temperature at a primary energy of 65 eV (dots). The solid line is a fit according to Eq. (1) with $T_c=754$ K, $C=0$, $B_+$, and $B_-$ variable, $\alpha_-=\alpha_+$, resulting in $\alpha=0.64$. Data above 780 K and between 750 and 758 K were excluded from the fit.

a Debye-Waller factor (in high-temperature approximation), which we determined from measurements down to 150 K so that the divided LEED intensity, extrapolated to 0 K, has a horizontal tangent there. If we insert the mass of a single Ru atom, the effective Debye temperature, $\Theta_D$, under these conditions is 300 K. It would be 750 K, if the mass of a single O atom is used, much higher than the Ru bulk Debye temperature of 420 K.[41] Though uncertainties in $\Theta_D$ are of the order of $\pm 10\%$, it is interesting to note, that the vibrational amplitudes of oxygen, compared to those of the Ru atoms, are essentially invisible in the Debye-Waller factor. This can be taken as another indication for a steep, site-specific adsorption potential with high activation barriers for diffusion, consistent with the activation needed for perfect ordering. It may be due to a slight reconstruction of the Ru surface by oxygen at this coverage, as indicated by dynamical LEED-*IV* analysis.[42]

The inflection point of the graph corresponds to $T_{c,\max}$ of $754 \pm 0.5$ K. As explained in Sec. III B, data very close to $T_c$ and far away from $T_c$ have to be excluded from the fit. Close to $T_c$ the fit deviates from the data in a range of $|t| < 0.005$, which we attribute, at least in part, to finite-size rounding, as the normalized slope $I^{-1}dI/dt = 51$ at $T_c$, instead of infinity. Therefore, we excluded this data range from the fitting procedure. At still higher temperatures, the fit had to be limited to 25 K above $T_c$ as the spot profile width approaches the size of the Faraday cup. This limits the validity of Eq. (1) at large $t$, as the Faraday cup is no longer effectively integrating over all short-range correlations. As will be seen below, contributions to superstructure beam intensities of short-range fluctuations below $T_c$ are very small so that the fit can be extended to a larger $t$ range below $T_c$.

The fits were carried out with increasing numbers of fitted parameters. With $C$ set to zero and $T_c$ fixed, $B_+ = B_-$, and $\alpha_+ = \alpha_-$, we obtain $\alpha = 0.60 \pm 0.04$. The error bar is due to shifts in $T_c$ by $\pm 1$ K and to variations of the excluded range from 0 to 0.01 $T_c$. If under the same conditions $B_+$ and $B_-$ are fitted independently, a ratio $B_+/B_- = 1 \pm 0.05$ is obtained. If the condition $\alpha_+ = \alpha_-$ is removed, they vary in the range between 0.58 and 0.65. A fixed positive value of $C$ tends to increase $\alpha$, but worsens the fit. Allowing $C$ as an additional fit parameter always drives $C$ negative, and makes the fitted curve more asymmetrical around $T_c$, with ratios $B_-/B_+$ up to 3. $\alpha$ is then systematically shifted to lower values by up to 10% of the average value. Changes in the fitted temperature range, which can be done over a larger $t$ range only below $T_c$, also influence the value of $\alpha$. Fits without linear correction terms result in a decrease of $\alpha$ by as much as 10%, if the upper cutoff in $|t|$ is reduced from 0.1 to 0.02, as can be directly seen from Fig. 2.

All values determined for $\alpha$ fall systematically below the theoretical value for $\alpha$ of the four-state Potts model ($\alpha = \frac{2}{3}$). This is also indicated in Fig. 2, where experimental data are compared to a straight line with slope $(1-\alpha) = \frac{1}{3}$ in a log-log plot. In addition, this figure clearly shows deviations from a simple power law. As there is no range in $t$ where the experimental curves are straight

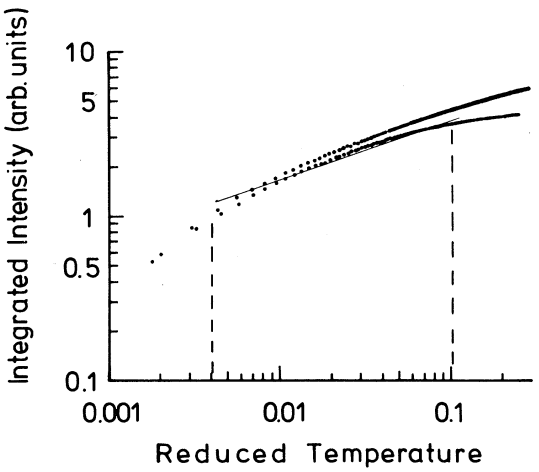


FIG. 2. The data of Fig. 1 plotted on double logarithmic scale vs reduced temperature. Lower-data set corresponds to $T > T_c$, upper set to $T < T_c$. The solid line indicates a power law $\sim |t|^{1-\alpha}$ with $(1-\alpha) = \frac{1}{3}$.

lines, these deviations cannot be caused by stretching the validity of Eq. (1). It clearly demonstrates that corrections to scaling are not negligible, though our fits seem to describe the data reasonably well on a linear scale. From the analysis above we have to conclude that higher-order correction terms are required to describe the data adequately. Our analysis, however, also shows that for our experimental system the simple power-law fit can be used as an indication that the phase transition observed belongs to the universality class of the four-state Potts model, to which the determined exponents are closest. Because of the large differences in the specific-heat exponents $\alpha$ between different universality classes, this method may be generally useful to discriminate between various universality classes.

A typical example of the peak intensity at $\Theta = 0.25$, measured with a small aperture in the Faraday cup, which integrates only over 0.05% of the Brillouin zone, versus reduced temperature $t$ is shown as a log-log plot in Fig. 3 (the same Debye-Waller factor as above has been divided out). Critical temperatures, as determined by the inflection points with small and big apertures in the Faraday cup, coincide within 1 K, as expected, because very close to $T_c$ the small aperture is also integrating over all correlations and Eq. (1) should be applicable for the small aperture as well. If not concealed by finite-size effects, crossover to behavior according to Eq. (2) should be observable. From our data we conclude that this must occur far below $t = 10^{-3}$: Using the $T_c$ measured with the small aperture, we plotted in Fig. 3 the *raw* data, i.e., without deconvolution, thus neglecting the second term of Eq. (2) below $T_c$ completely. From such plots we obtain a slope $2\beta = 0.17 + 0.03/-0.01$, which compares well with the theoretical value of $\frac{1}{6}$. The perfect fit to a straight line also indicates very small critical scattering for $t < 0$, which we cannot even identify from our mea-

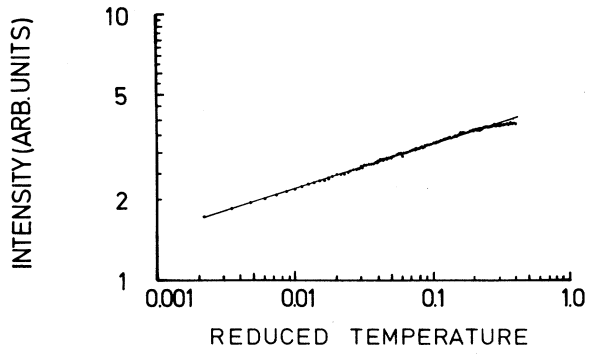


FIG. 3. Peak intensity below $T_c$ of a second-order oxygen induced spot as a function of reduced temperature after division by a Debye-Waller factor. Slope of solid-straight line $2\beta=0.17$.

surements in the accessible $t$ range. The error limits are again mainly due to uncertainties in fixing $T_c$, with a smaller contribution from fixing the diffuse background.

Above $T_c$, the beam profiles broaden and decrease in magnitude as critical scattering decays. These profiles were fitted according to Eq. (2) with the convolution procedure described in the previous section. A typical profile above $T_c$ together with the fit is shown in Fig. 4. As a result of the fit, $I_0$ is nonzero for $t<0.004$, which can be partly due to finite-size rounding. The deconvoluted peak intensity and the inverse beam width at half maximum (corresponding to the correlation length $\xi$) are plotted in Fig. 5 as a function of reduced temperature for different electron energies and beam orders, taking the same values of $T_c$ as for the $\beta$ determination. Note that in Ref. 34, the scale for $\xi$ was erroneously a factor of 3 too large. It is corrected here, which, however, only leads a parallel shift of the data and does not change exponents. On these log-log plots the data can again be

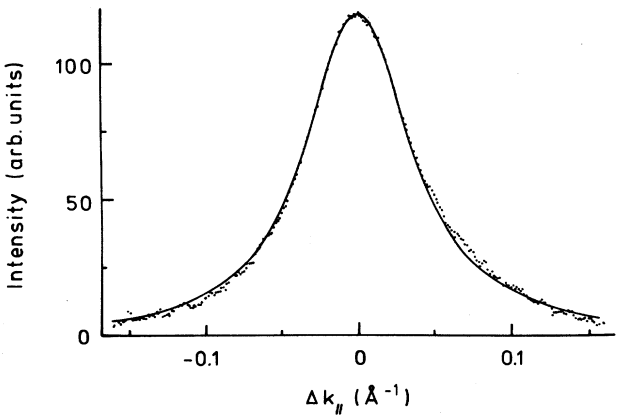


FIG. 4. Comparison of a second-order superstructure beam profile at a primary energy of 65 eV for reduced $t=0.008$ ($T=760$ K) after subtraction of a linear background with the result of the fitting procedure convoluting Eq. (2) with the instrument function (solid line), as described in the text.

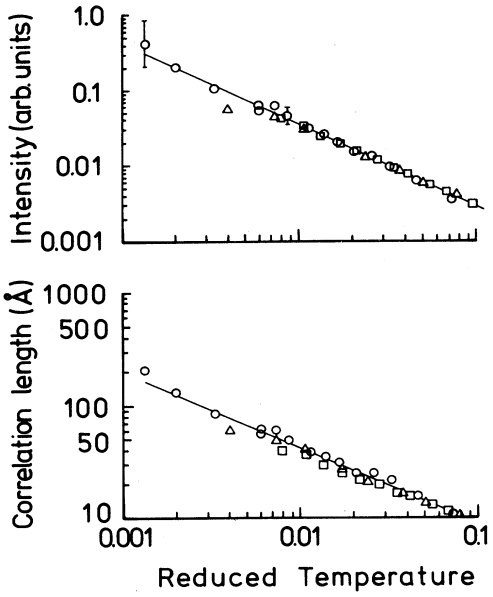


FIG. 5. Deconvoluted peak height of critical scattering $\chi_0$ and inverse full widths at half maximum (correlation lengths $\xi$) above $T_c$. Different symbols correspond to different energies and diffraction orders: first order at 52 eV (squares), second order at 36.5 eV (circles) and at 65 eV (triangles). Amplitudes in the upper figure are normalized with respect to the data set at 65 eV.

well fitted to straight lines which yield the exponents $\gamma=1.08\pm0.07$ and $\nu=0.68\pm0.03$. They both are in close agreement with the theoretical four-state Potts exponents. The accuracy for determining these exponents, especially at small $t$, is mainly limited by instrument resolution, i.e., by small variations of the low-temperature profile shape corresponding to variations in halfwidth of $\Delta k_{\parallel}=1.5\times10^{-3}$ Å$^{-1}$. They affect our determination of the "instrument function," which also contains contributions from crystal imperfections such as mosaic spread, etc. The upper limit in $t$ is due to small signals and beam profiles so broad that the atomic structure of the surface becomes more and more important, and deviations from isotropically round profiles have to be expected.[38] Thus for the determination of exponents, we are limited to roughly 1.5 orders of magnitude in reduced $t$. Finite-size effects, though clearly visible in Fig. 1, cannot be discriminated in Fig. 5 within the uncertainties indicated. The exponents are summarized in Table I, together with theoretical values of various $n$-state Potts universality classes.[43] Agreement with the values of the four-state Potts universality class within 3–10 % is obtained.

## IV. DISCUSSION

The characterization of a phase transition as continuous under the condition of constant coverage is not always reliable if simply based on the continuous disap-

TABLE I. Summary of experimental and comparison with theoretical (Ref. 44) critical exponents of two-dimensional universality classes.

| | Experiment | four-state Potts | three-state Potts | Ising |
|---|---|---|---|---|
| $\alpha$ | 0.60 $\pm$0.04 | 0.667 ($\frac{2}{3}$) | 0.333 ($\frac{1}{3}$) | 0 (log) |
| $\beta$ | $0.085^{+0.015}_{-0.005}$ | 0.083 ($\frac{1}{12}$) | 0.111 ($\frac{1}{9}$) | 0.125 ($\frac{1}{8}$) |
| $\gamma$ | 1.08 $\pm$0.07 | 1.167 ($\frac{7}{6}$) | 1.444 ($\frac{13}{9}$) | 1.75 ($\frac{7}{4}$) |
| $\nu$ | 0.68 $\pm$0.03 | 0.667 ($\frac{2}{3}$) | 0.833 ($\frac{5}{6}$) | 1 |

pearance of superstructure beam intensities as a function of temperature and on the lack of hysteresis effects. Hysteresis can be suppressed by finite-size effects,[44] a problem one always has to cope with in 2D, as discussed below. For constant coverage, i.e., for constant number of particles on the surface, melting of islands in a mixed phase of islands and lattice gas is a continuous process. This was demonstrated experimentally for several examples, one of them being CO/Ru(001) (Ref. 13), and a distinction between first and higher-order phase transitions based solely on such measurements is doubtful. For the case investigated here, however, the determination of critical exponents and their good agreement with one of the possible universality classes is a clear indication of a continuous phase transition.

As mentioned in the Introduction, we not only need knowledge about the ordered, but also the disorder phase in order to characterize the symmetry change during the phase transition. For our system to belong to the four-state Potts universality class, it is necessary that the oxygen atoms occupy the same high-symmetry site (on top or threefold site) in ordered and disordered phase. This assumption of a lattice gas needs to be checked, however. Cluster calculations by Anderson and Awad[45] for oxygen on Ru(001) favor the threefold-coordinated fcc site (no atom below in the second Ru layer) by 0.3 eV over the hcp site. This contradicts our structural investigation by LEED-*IV* analysis for the ordered $p(2\times2)$ phase, which favors the hcp site,[42] as mentioned. Clear experimental evidence for a lattice gas also in the disordered phase comes from very-low-energy electron diffraction (VLEED).[46] For electron incidence close to the surface normal the (00) beam intensity as a function of electron energy reacts very sensitively to adsorbates and their site symmetry, but only sightly to the environment in the adlayer, as tested by model calculations.[47] Especially for the case of O/Ru(001), we find no change of the *I-V* curve of the (00) beam in the range 7–32 eV when going through the phase transition of the $p(2\times2)$ structure.[48] From that we conclude that also in the disordered phase oxygen occupies the same site as in the ordered phase with high preference which, according to our LEED-*IV* analysis, is the hcp site. Therefore, the geometrical preconditions for the observation of exponents within the four-state Potts universality class seem to be fulfilled.

Our experiments are a clear example of the feasibility of a moderately accurate determination of critical exponents for two-dimensional systems, which is limited by finite-size effects and, in our case, also by instrument resolution. The latter does not allow us to give precise limits where finite-size rounding sets in. Nevertheless, the good power-law behavior over 1.5–2 orders of magnitude in reduced temperature, though restricted to a range $t > 10^{-3}$, gives confidence in the determination of the critical exponents $\beta$, $\gamma$, and $\nu$ within 10% of the average value. Towards the small-$t$ side it demonstrates that we are outside the $t$ range where finite-size effects are important. The good agreement with the theoretical four-state Potts values can be taken as evidence that we have found a two-dimensional system which belongs to this universality class. Smaller $t$ ranges, used in most other determinations of two-dimensional critical exponents reported in the literature, consequently increase the uncertainty of determination and might not even allow one to separate out contributions due to imperfections.

The influence of strong multiple-scattering effects on reliable determinations of critical exponents was a matter of recent discussion in the literature.[49,50] Multiple scattering cannot influence determinations of exponents $\alpha$ (multiple-scattering effects included, see above) and $\beta$.[50] As multiple scattering is short ranged, it also will not preclude scaling of short-range order correlations if the correlation length is much larger than the typical range of multiple scattering.[50] Our experimental findings corroborate this argument, though multiple-scattering contributions within the adsorbate layer are minimized in our experiments because they are carried out at normal incidence.

The restricted range in reduced temperature $t > 10^{-3}$ also raises the question of corrections to scaling. In the four-state Potts universality class these should be particularly important, because power-law corrections for the order parameter are expected to have a logarithmic leading term.[51] Such nonuniversal corrections are clearly seen in model calculations.[38] Critical scattering of short-range fluctuations should also contribute to the measured intensity below $T_c$. From the perfect fit of the raw data to a power law below $T_c$ in our experiment, we conclude that both contributions do not vary by more than a few percent over the measured $t$ range. Compared especially with the Monte Carlo simulations carried out in Ref. 38, nonlinear corrections to scaling are vanishingly small, thus emphasizing their nonuniversal character. As amplitude ratios are universal,[3] it is also not surprising to find no contributions of critical scattering below $T_c$ in the measured $t$ range: In Ref. 38 these ratios for $\xi_+/\xi_-$ and $\chi_{0+}/\chi_{0-}$ were determined as 3.9$\pm$0.9 and 39$\pm$15, respectively. Taking the ratio for the amplitudes we expect

a contribution of 7% at $t=0.002$, the data point closest to $T_c$ in Fig. 4. Above $T_c$, small corrections to scaling cannot be excluded, especially for the critical exponent $\gamma$, as we can, strictly speaking, only determine effective exponents[3,38] over a limited $t$ range, which also depend on the exact value of $T_c$. The systematically too small values for $\gamma$ may be an indication. Such corrections would also change $T_c$ within the uncertainties of its determination.

The use of integrated intensities to determine the exponent $\alpha$, where the largest deviations from simple power-law behavior were observed, was not only suggested but also extensively simulated for conditions similar to our experiment by Bartelt *et al.*[37] Very similarly to our experiment, they find exponents systematically 10% below the theoretical value for simple power-law form. In agreement with our findings a linear term increases the discrepancy. The calculated behavior of internal energy, however, exactly follows the calculated intensity. Therefore, the discrepancy to simple power-law form must be due to higher-order corrections, neglected both in the model calculations and in our data analysis. Even with a power-law fit, however, we can conclude from our data that a discrimination between different universality classes is clearly feasible, if the existence of a continuous phase transition can be proven otherwise. The method itself certainly contains valuable additional information, which needs further systematic investigations.

## V. CONCLUSIONS

We have shown that fairly reliable determinations of critical exponents in 2D are possible, if adsorption sites of the ordered as well as the disordered phase are known. For the system O/Ru(001), which orders in a $p(2\times2)$ structure on hcp threefold sites, we determined the exponents $\alpha$, $\beta$, $\gamma$, and $\nu$ independently in the temperature range $4\times10^{-3}<t<0.1$. They agree within 3–10 % with the exponents of the four-state Potts universality class. Corrections to scaling were shown to be small for this system so that they affect exponent determinations in the $t$ range accessible very little. This property, however, is nonuniversal, so that in general a closer approach to $T_c$ is desirable. The integrated intensity exhibits fairly large deviations from power-law behavior, but still can be used as a first test of the universality class.

## ACKNOWLEDGMENTS

We thank U. Höfer for support in numerical problems and D. Menzel for a critical reading of the manuscript. Financial support from the Natural Sciences and Engineering Research Council of Canada for one of us (P.P.) is also gratefully acknowledged. This work was funded by the Deutsche Forschungsgemeinschaft through Sonderforschungsbereich 128.

*Present address: University of Ottawa, Ottawa, Ontario, Canada K1N 6N5.

[1]See, e.g., Surf. Sci. **125** (1983).
[2]D. P. Landau, in *Monte Carlo Methods in Statistical Physics,* edited by K. Binder (Springer-Verlag, Berlin, 1986), p. 337.
[3]T. L. Einstein, in *Proceedings of the 10th Johns Hopkins Workshop, Bad Honnef, 1986,* edited by K. Dietz and V. Ritterberg (World Scientific, Singapore, 1987), p. 17.
[4]H. E. Stanley, *Introduction to Phase Transitions and Critical Phenomena* (Oxford University Press, New York, 1971).
[5]K. G. Wilson, Phys. Rep. **12**, 75 (1974).
[6]D. P. Landau and E. M. Lifschitz, *Lehrbuch der Theoretischen Physik* (Akademie Verlag, Berlin, 1966), Vol. 5, p. 462 ff.
[7]M. Schick, Prog. Surf. Sci. **11**, 245 (1981).
[8]E. Domany, M. Schick, J. S. Walker, and R. B. Griffiths, Phys. Rev. B **18**, 2209 (1978); C. Rottman, *ibid.* **24**, 1482 (1981).
[9]M. A. Van Hove, W. H. Weinberg, and C. M. Chan, *Low Energy Electron Diffraction, Experiment, Theory and Surface Structure Determination* (Springer-Verlag, Berlin, 1986).
[10]G. A. Somorjai and M. A. Van Hove, *Adsorbed Monolayers on Solid Surfaces* (Springer-Verlag, Berlin, 1979).
[11]J. C. Campuzano, M. S. Foster, G. Jennings, R. F. Willis, and W. N. Unertl, Phys. Rev. Lett. **54**, 2684 (1985); J. C. Campuzano, G. Jennings, and R. F. Willis, Surf. Sci. **162**, 484 (1985).
[12]D. E. Clark, W. N. Unertl, and P. H. Kleban, Phys. Rev. B **34**, 4379 (1986).
[13]H. Pfnür and D. Menzel, Surf. Sci. **148**, 411 (1984).
[14]G. C. Wang and T. M. Lu, Phys. Rev. B **31**, 5918 (1985).
[15]I. F. Lyuksyutov and A. G. Fedorus, Zh. Eksp. Teor. Fiz. **80**, 2511 (1981) [Sov. Phys.—JETP **53**, 1317 (1981)].
[16]J. F. Wendelken and G. C. Wang, Phys. Rev. B **32**, 7542 (1985).
[17]L. D. Roelofs, A. R. Kortan, T. L. Einstein, and R. L. Park, Phys. Rev. Lett. **46**, 1465 (1981).
[18]M. Tejwani, O. Ferreira, and O. E. Vilches, Phys. Rev. Lett. **40**, 152 (1980).
[19]H. K. Kim and M. H. W. Chan, Phys. Rev. Lett. **53**, 170 (1984).
[20]J. H. Campbell and M. Bretz, Phys. Rev. B **32**, 2861 (1985).
[21]K. D. Miner, M. H. W. Chan, and A. D. Migone, Phys. Rev. Lett. **51**, 1465 (1983); A. D. Migone, M. H. W. Chan, K. J. Niskanen, and R. B. Griffiths, J. Phys. C **16**, L1115 (1983).
[22]H. Freimuth and H. Wiechert, Surf. Sci. **162**, 432 (1985).
[23]T. E. Madey, H. A. Engelhardt, and D. Menzel, Surf. Sci. **48**, 304 (1975).
[24]J. C. Fuggle, T. E. Madey, M. Steinkilberg, and D. Menzel, Surf. Sci. **52**, 521 (1975).
[25]G. E. Thomas, W. H. Weinberg, J. Chem. Phys. **70**, 954 (1979).
[26]T. S. Rahman, A. B. Anton, N. R. Avery, and W. H. Weinberg, Phys. Rev. Lett. **51**, 1979 (1983).
[27]H. I. Lee, G. Praline, and J. M. White, Surf. Sci. **91**, 581 (1980); S. K. Shi, and J. M. White, J. Chem. Phys. **73**, 5889 (1980).
[28]L. Parrot, G. Praline, B. E. Koel, J. M. White, and T. N. Taylor, J. Chem. Phys. **71**, 3352 (1979).
[29]L. Surnev, G. Rangelov, and G. Bliznakov, Surf. Sci. **159**, 299

(1985).
[30]E. Umbach, Ph.D. dissertation, Technische Universität, München, 1980 (unpublished).
[31]P. Piercy, M. Maier, and H. Pfnür, in *The Structure of Surfaces II,* edited by J. F. van der Veen and M. A. Van Hove (Springer-Verlag, Berlin, 1988), p. 480.
[32]P. Piercy and H. Pfnür (unpublished).
[33]M. E. Fisher, Phys. Rev. **176**, 257 (1968).
[34]P. Piercy and H. Pfnür, Phys. Rev. Lett. **59**, 1124 (1987).
[35]M. Sokolowski and H. Pfnür, Phys. Rev. Lett. (to be published).
[36]M. N. Barber in *Phase Transitions,* edited by C. Domb and J. L. Lebowitz (Academic, London, 1983), Vol. 8, p. 145.
[37]N. C. Bartelt, T. L. Einstein, and L. D. Roelofs, Surf. Sci. **149**, L47 (1985); Phys. Rev. B **32**, 2993 (1985).
[38]N. C. Bartelt, T. L. Einstein, and L. D. Roelofs, Phys. Rev. B **35**, 1776 (1987).
[39]P. Pfeuty and G. Toulouse, *Introduction to the Renormalization Group and to Critical Phenomena,* (Wiley, London, 1977).
[40]*Numerical Data and Functional Relationships in Science and Technology, New Series,* Vol. IV/2b of *Landolt-Bornstein,* edited by K. H. Hellwege (Springer-Verlag, Berlin, 1982).
[41]*International Tables for X-Ray Crystallography Vol. III,* (Kynoch, Birmingham, 1968), p. 239.
[42]M. Lindroos, H. Pfnür, G. Held, and D. Menzel, Surf. Sci. (to be published).
[43]F. Y. Wu, Rev. Mod. Phys. **54**, 235 (1982); M. P. M. den Nijs, J. Phys. A **12**, 1857 (1979); B. Nienhuis, E. K. Riedel, and M. Schick, *ibid.* **13**, L189 (1980); R. B. Pearson, Phys. Rev. B **22**, 2579 (1980).
[44]O. G. Mouritsen, *Computer Studies of Phase Transitions and Critical Phenomena* (Springer-Verlag, Berlin, 1984).
[45]A. B. Anderson and M. K. Awad, Surf. Sci. **183**, 289 (1987).
[46]M. Lindroos, H. Pfnür, and D. Menzel, Phys. Rev. B **33**, 6684 (1986).
[47]M. Lindroos, H. Pfnür, and D. Menzel, Surf. Sci. **192**, 421 (1987).
[48]H. Pfnür, M. Lindroos, and D. Menzel (unpublished).
[49]W. Moritz and M. G. Lagally, Phys. Rev. Lett. **56**, 865 (1986).
[50]N. C. Bartelt, T. L. Einstein, and L. D. Roelofs, Phys. Rev. Lett. **56**, 2881 (1986).
[51]J. L. Cardy, M. Nauenberg, and D. J. Scalapino, Phys. Rev. B **22**, 2560 (1980).